

# Soliton in BCS superfluid Fermi gas

Jacek Dziarmaga and Krzysztof Sacha

*Instytut Fizyki Uniwersytetu Jagiellońskiego, ul. Reymonta 4, 30-059 Kraków, Poland*  
(June 23, 2004)

We analyze a superfluid state of two species gas of fermions trapped in a quasi-1D harmonic potential and interacting via attractive s-wave collisions. It is shown that the gap equation possesses a self consistent solution with an antisymmetric gap function. The gap function has a localized soliton or kink in the center of the trap.

03.65.-w, 03.75.Fi, 42.50.Md

Over the last decade we experienced rapid development in trapping and cooling of dilute atomic gases that made condensates of bosonic atoms standard objects of investigation in laboratories of atomic physics [1]. At the same time transition to a superfluid state in cold fermionic gases seems to be already attainable [2–4]. The remarkable level of manipulation and control of dilute bosonic gases allowed for a number of spectacular experiments with Bose-Einstein condensates (BEC) [1]. Similar experimental activity in fermionic superfluidity may be expected in the immediate future.

In the present Letter we investigate superfluid phase of a two-species fermionic gas in the weak coupling BCS regime trapped in a quasi one-dimensional (1D) harmonic trap. The presence of a trapping potential is a necessary condition to have superfluidity in an effective one dimensional system. We show that the gap function can have a soliton. Dark solitons in a 1D Bose-Einstein condensate have been investigated theoretically and experimentally for a few years [5,6]. Atomic density drops to zero in the dark soliton. In contrast, the quasi 1D Fermi superfluid can support a soliton that does not show up in the density distribution but only in the gap function.

Two species of Fermions  $\hat{\psi}_-(x)$  and  $\hat{\psi}_+(x)$  with an attractive mutual s-wave interactions in a quasi-1D harmonic trap are described by the Hamiltonian

$$\hat{H} = \int_{-\infty}^{+\infty} dx \left[ \hat{\psi}_+^\dagger \mathcal{H}_0 \hat{\psi}_+ + \hat{\psi}_-^\dagger \mathcal{H}_0 \hat{\psi}_- - g \hat{\psi}_-^\dagger \hat{\psi}_+^\dagger \hat{\psi}_+ \hat{\psi}_- \right].$$

Here  $\mathcal{H}_0 = -\frac{1}{2} \frac{\partial^2}{\partial x^2} + \frac{1}{2} x^2 - \mu$  is the single particle Hamiltonian in the trap units.  $g > 0$  is an effective 1D strength of attraction. In the usual BCS mean-field approximation with the pairing field  $\Delta(x) = g \langle \hat{\psi}_+(x) \hat{\psi}_-(x) \rangle$  and the Hartree-Fock potential  $W(x) = -g \langle \hat{\psi}_\pm^\dagger(x) \hat{\psi}_\pm(x) \rangle$  the stationary problem at zero temperature is equivalent to solving the Bogoliubov-de Gennes equations [7]

$$\begin{aligned} \omega_m u_m &= +\mathcal{H}_0 u_m + W(x) u_m + \Delta(x) v_m, \\ \omega_m v_m &= -\mathcal{H}_0 v_m - W(x) v_m + \Delta^*(x) u_m, \end{aligned} \quad (1)$$

together with the self-consistency conditions

$$\Delta(x) = g \sum_{m=1}^{\infty} u_m(x) v_m^*(x), \quad (2)$$

$$W(x) = -g \sum_{m=1}^{\infty} |v_m(x)|^2. \quad (3)$$

Unlike in 2D or 3D [8,9], in 1D both sums are convergent. Similar Bogoliubov-de Gennes equations with soliton solutions appear in the theory of conducting polymers [10] where the order parameter  $\Delta$  is real and lives on a discrete 1D lattice.

In numerical calculations the infinite sums must be replaced by finite sums up to a certain cut-off  $\Lambda$ ,

$$\Delta_\Lambda(x) = g \sum_{m=1}^{\Lambda} u_m(x) v_m^*(x). \quad (4)$$

For a sufficiently large cut-off  $\Delta_\Lambda(x)$  converges to  $\Delta(x)$ . In principle for fixed  $(u_m, v_m)$  the difference is  $\Delta(x) - \Delta_\Lambda(x) = \mathcal{O}(\Lambda^{-1/2})$ . Unfortunately, we found that the small error  $\mathcal{O}(\Lambda^{-1/2})$  was amplified by the nonlinear set of Eqs.(1)-(3) and the convergence was much slower. This is why we use a different prescription

$$\Delta(x) = \Delta_\Lambda(x) + \delta\Delta_\Lambda(x). \quad (5)$$

Here  $\delta\Delta_\Lambda(x) \approx g \sum_{m=\Lambda+1}^{\infty} u_m(x) v_m^*(x)$  is an approximate analytical expression for the part of the infinite sum that is normally ignored. Again for  $\Lambda$  large enough we recover the infinite sum, but now the convergence is much faster than for the simple cut-off in Eq.(4).

We use the local density approximation (LDA) to evaluate the high energy part of the gap function

$$\delta\Delta_\Lambda(x) = g \int_{|k| > k_\Lambda(x)} \frac{dk}{2\pi} \frac{\Delta(x)}{2E(k, x)}. \quad (6)$$

In the LDA the superfluid is considered locally uniform so that locally one can use the BCS theory for a uniform system. In equation (6) the  $E(k, x) = \sqrt{\Delta^2(x) + \epsilon^2(k, x)}$  is a local quasiparticle energy with  $\epsilon(k, x) = \frac{k^2}{2} + \frac{x^2}{2} + W(x) - \mu$ . A local cut-off momentum  $k_\Lambda(x)$  corresponding to the cut-off energy  $\omega_\Lambda + \mu$  is given by  $k_\Lambda^2(x) = 2\omega_\Lambda + 2\mu - x^2 - 2W(x)$  when positive and zero otherwise. A combination of Eqs.(5) and (6) gives to leading order in  $\Delta(x)$

$$\Delta(x) \approx g_\Lambda(x) \sum_{m=1}^{\Lambda} u_m(x) v_m^*(x), \quad (7)$$

$$\frac{1}{g_\Lambda(x)} \stackrel{\text{def.}}{=} \frac{1}{g} - \frac{1}{2\pi} \int_{k_\Lambda(x)}^{\infty} \frac{dk}{2E(k,x)}$$

$$\approx \frac{1}{g} - \frac{1}{2\pi k_F(x)} \ln \left( \frac{k_\Lambda(x) + k_F(x)}{k_\Lambda(x) - k_F(x)} \right).$$

Here  $k_F(x) = \sqrt{2\mu - x^2 - 2W(x)}$  is a local Fermi momentum. The LDA applied to the highest quasiparticle states results in an  $x$ -dependent attraction strength  $g_\Lambda(x)$ . The enhanced  $g_\Lambda(x) > g$  approximately compensates for the high energy quasiparticle states missing in the finite sum. We use the LDA to evaluate only the sum  $\delta\Delta_\Lambda(x)$  over the high energy states. Although accuracy of LDA as such may be disputable, there is little doubt that it is a very accurate approximation in the high energy regime where  $k_\Lambda(x)$  is much greater than any rate of variation of  $\Delta(x)$ .

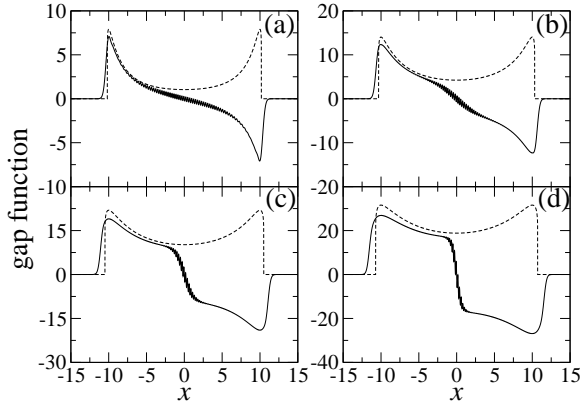


FIG. 1. Gap functions  $\Delta(x)$  in the antisymmetric state (solid lines) and approximate LDA gap functions  $\Delta_{\text{LDA}}(x)$  in the symmetric ground state (dashed lines) for  $g = 6$  [panel (a)],  $g = 8$  [panel (b)],  $g = 10$  [panel (c)], and  $g = 12$  [panel (d)]. The chemical potential is  $\mu = 50$  which gives an average total number of atoms ranging from  $2 \times 70$  for  $g = 6$  to  $2 \times 82$  for  $g = 12$ .

In this paper we consider an antisymmetric  $\Delta(x) = -\Delta(-x)$  with a symmetric density of atomic cloud  $W(x) = W(-x)$  in the weak coupling BCS regime. The solid lines in Fig.1 show the antisymmetric gap functions for four values of the attraction strength  $g$ . Panels (b)-(d) show very clear characteristic soliton (kink) patterns, but in panel (a) the width of the soliton is comparable to the size of the atomic cloud and we see just a plain antisymmetric state.

The dashed lines in Fig.1 show symmetric ground state  $\Delta(x)$ 's obtained with the LDA. To get this approximate

gap function we set  $\Lambda = 0$  on the left hand side of Eq.(6) which replaces the  $\delta\Delta_\Lambda(x)$  by an approximate  $\Delta(x)$ . Then we solve Eq.(6) to leading order in  $\Delta(x)$ :

$$\Delta_{\text{LDA}}(x) = 4 k_F^2(x) e^{-\pi k_F(x)/g} \quad (8)$$

wherever  $k_F(x)$  is real and 0 otherwise. The agreement between the symmetric  $\Delta_{\text{LDA}}$  and modulus of antisymmetric gap functions is reasonable even for the small numbers of atoms considered in Fig.1. The solitons in panels (b)-(d) can be considered as localized defects in a locally uniform superfluid.

The gap function  $\Delta(x)$  has a soliton but, unlike for dark solitons in BEC [5,6], corresponding atomic density shows hardly any symptoms of the soliton at all, see Fig.2. The soliton in the weakly interacting BCS superfluid is not a dark soliton.

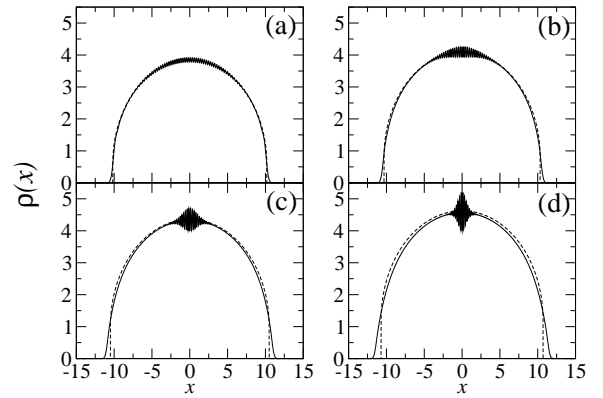


FIG. 2. Atomic densities  $\rho(x) = \langle \hat{\psi}_\pm^\dagger(x) \hat{\psi}_\pm(x) \rangle$  corresponding to the antisymmetric states in Fig.1. The fast oscillations of  $\rho(x)$  in the solitons average to zero on length scales longer than  $k_F^{-1}$ . The dashed plots show approximate  $\rho_{\text{LDA}} = \frac{g}{\pi^2} + \frac{1}{\pi} \sqrt{2\mu - x^2 + \frac{g^2}{\pi^2}}$ .

To demonstrate convergence of the scheme based on Eq. (7) we show  $\Delta(x)$  for  $g = 12$  and increasing value of  $\Lambda$  in Fig.3. In this figure we also show results corresponding to Eq. (4) where the contributions from the high energy states are neglected. We see that the results based on the scheme Eq. (7) are closer to the true solution, even for  $\Lambda = 400$ , than those based on the simple cut-off scheme (4) with  $\Lambda = 1000$ .

We need some analytical insights to extrapolate the numerical results to a large number of atoms  $N$ . The most intriguing issue is the width of the soliton. A simple estimate of the healing length  $\xi$  can be obtained in the LDA. The local quasiparticle energy  $E(k, x)$  can be

expanded in small fluctuations  $\delta k = k - k_F$  around Fermi momentum

$$E = \sqrt{\Delta^2 + \left(\frac{k^2 - k_F^2}{2}\right)^2} \approx k_F \sqrt{\frac{\Delta^2}{k_F^2} + \delta k^2}. \quad (9)$$

We see that the quasiparticle spectrum is affected by the gap only in the range of  $\delta k \approx \Delta/k_F$ . This is the dispersion of momenta available to construct a localized soliton and so the healing length must scale as

$$\xi = \alpha \frac{\sqrt{2\mu}}{\Delta} \quad (10)$$

with a constant  $\alpha = \mathcal{O}(1)$ . To estimate the constant we fit the solitons in panels (b)-(d) in Fig.1 with a trial function  $\gamma\Delta_{\text{LDA}}(x)\tanh(x/\xi)$ , where  $\gamma$  and  $\xi$  are fitting parameters. The best fit to the central part of panel (d) is shown in Fig.4. From  $\xi$ 's we obtain the best fits for  $\alpha$ 's and show them in Table I — it is fair to say that  $\alpha \approx 1$ .

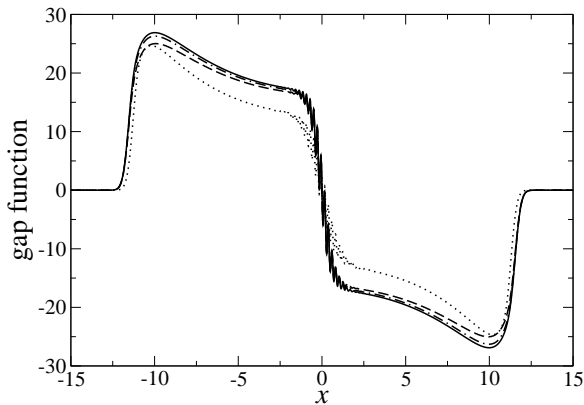


FIG. 3. Gap functions calculated in different approximations for chemical potential  $\mu = 50$  and attraction strength  $g = 12$ . Dotted line corresponds to Eq. (4) with  $\Lambda = 1000$ . Dashed, dotted-dashed and solid lines are the results that base on Eq. (7) with  $\Lambda$  equal to 400, 700 and 1000, respectively.

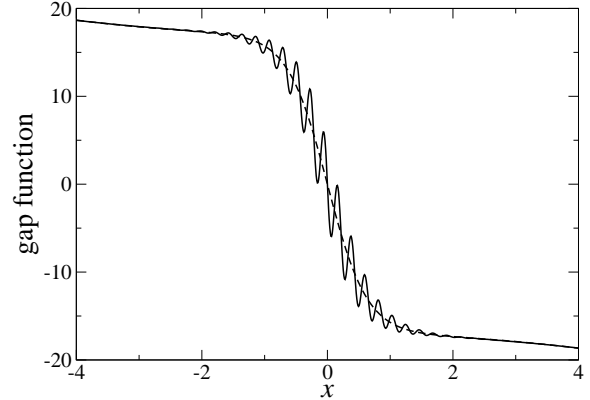


FIG. 4. Solid line indicates the gap function shown in panel (d) of Fig. 1. Dashed line is a fit to the solid line with a trial function  $\gamma\Delta_{\text{LDA}}(x)\tanh(x/\xi)$  performed in the range of space presented in the figure only. The best fit was obtained for  $\alpha = 1.07$ , Eq. (10).

Another interesting question is when the soliton is a nice localized kink as in panels (b)-(d) of Fig.1 and when its width is comparable or exceeds the width of the atomic cloud as in panel (a). A simple estimate of the “kinkness” of the antisymmetric state is the ratio of the healing length to the Thomas-Fermi width of the cloud  $x_{\text{TF}} \approx \sqrt{2\mu}$ ,

$$\frac{\xi}{x_{\text{TF}}} \approx \frac{1}{\Delta}. \quad (11)$$

This factor can be made small for large  $N$  when a large  $\Delta \gg 1$  is easily compatible with the weak coupling condition  $\Delta \ll \mu$  necessary for the LDA to be accurate.

Once we have a localized soliton another interesting question arises. A localized soliton should behave like a non-dispersive point particle. As the atomic cloud in the trap is non-uniform this particle feels an effective potential  $V_{\text{eff}}(q)$  with soliton position  $q$ . The question is what is the shape of this potential. This is an important issue related to stability because, for example, the dark solitons in BEC experience an inverted harmonic potential [5]. Their small fluctuation spectrum has an anomalous mode with negative frequency which might imply their instability. Fortunately, it does not for technical reasons specific to the dark solitons in harmonic traps. To get an insight into  $V_{\text{eff}}(q)$  we make a simple estimate of the soliton energy. According to Ref. [7] the difference between the energy density of the superfluid state with a gap  $\Delta \neq 0$  and the normal state with  $\Delta = 0$  is given by

$$\delta\varepsilon = \int_0^\Delta d\Delta' \left(\Delta'\right)^2 \frac{d g^{-1}}{d\Delta'}. \quad (12)$$

When combined with the LDA dependence of the gap on the attraction strength  $g$  in Eq.(8), this formula gives

$\delta\varepsilon = -\Delta^2/2\pi k_F$ . Now, in zero order approximation the soliton is an area of width  $\xi$  where this energy gain is missing, hence the energy of the soliton is roughly  $-\delta\varepsilon \times \xi$  or

$$V_{\text{eff}}(q) \sim |\Delta_{\text{LDA}}(x=q)|. \quad (13)$$

We come to a remarkably simple conclusion that the effective potential is proportional to the dashed plots in Fig.1. Small fluctuations of the soliton close to the minimum of the potential in the center of the trap have positive frequency. There is no anomalous mode that might imply thermodynamic instability. In order to deexcite the superfluid from the soliton state to the symmetric ground state the soliton has to be pushed beyond the potential barrier at the edge of the atomic cloud. In this sense solitons in the BCS Fermi superfluid are more robust than dark solitons in BEC. Hopefully the dark soliton experiments in BEC will find their counterpart in BCS Fermi superfluid.

As was shown in Ref. [11], in a 3D Fermi superfluid in an isotropic harmonic trap there is no energy gap in the quasiparticle energy spectrum even for a large gap function  $\Delta(\vec{x})$  in the center of the trap. Thus in 3D the spectroscopic detection of the BCS state requires the probing laser beam to be focused on the locally uniform central part of the trap. However, the detection schemes based on the measurement of the energy gap [12] can be very useful in 1D. In 1D a nonzero  $\Delta(x)$  directly translates into a gap in the quasiparticle spectrum.

What is more the same schemes can be used to detect the soliton in the superfluid. In Table II we list the lowest quasiparticle energies for the solitons in panels (c)-(d) of Fig.1. The energies  $\omega_{m>1}$  start roughly at the gap close to the center of the trap  $|\Delta(x \approx 0)|$ . This is the usual gap in the BCS state. However, the lowest  $\omega_1$  is an order of magnitude lower. This is a quasiparticle bound state localized inside the soliton where the gap function is close to zero. This mode is a soliton counterpart of the Caroli-de Gennes bound states inside a vortex core [13]. The bound state manifests itself in the density plots in Fig.2 by the fast density oscillations inside the soliton. The spectroscopic detection schemes will see the energy of the bound state in the soliton and they can be used both to detect the BCS state in 1D and to distinguish the ground state from the soliton state.

In conclusion, we have explored physics of soliton in superfluid atomic Fermi gases. Well defined kink-like soliton in the gap function can be obtained in a quasi-1D trap. We have estimated its width and energy and argued that small fluctuations of a soliton around the center of the trap have positive frequency. In this respect the BCS soliton is more robust than the dark soliton in a Bose-Einstein condensate. The soliton in superfluid fermi gases can be detected by spectroscopic measurements where the energy of the quasiparticle bound state localized in the soliton may be observed.

TABLE I. Values of  $\alpha$  parameter, Eq. (10), obtained from fitting of a trial function,  $\gamma\Delta_{\text{LDA}}(x)\tanh(x/\xi)$ , to the gap functions shown in panels (b)-(d) of Fig. 1.

Panel in Fig. 1	(b)	(c)	(d)
$\alpha$	1.07	1.05	1.07

TABLE II. The lowest quasiparticle energies for the solitons in panels (c)-(d) of Fig.1.

Panel in Fig. 1	(c)	(d)
$\omega_1$	1.9	4.0
$\omega_2$	11.5	20.1
$\omega_3$	11.7	20.3
$\omega_4$	13.0	21.4

**Acknowledgements.**— This work was supported in part by the the KBN grant PBZ-MIN-008/P03/2003.

---

- [1] J. R. Anglin and W. Ketterle, *Nature (London)* **416**, 211 (2002).
- [2] H.T.C. Stoof, M. Houbiers, C.A. Sackett, and R.G. Hulet, *Phys.Rev.Lett.***76**, 10 (1996); E. Timmermans, P. Tommasini, M. Hussein, and A. Kerman, *Phys.Rep.***315**, 199 (1999).
- [3] E. Timmermans, K. Furuya, P.W. Milonni, and A.K. Kerman, *Phys.Lett.A* 285 (2001); M. Holland, S.J.J.M.F. Kokkelmans, M.L. Chiofalo, and R. Walser, *Phys.Rev.Lett.***87**, 120406 (2001); S.J.J.M.F. Kokkelmans, G.V. Shlyapnikov, and C. Salomon, *cond-mat/0308384*.
- [4] C. A. Regal, M. Greiner, and D. S. Jin, *Phys. Rev. Lett.* **92**, 040403 (2003); M.W. Zwierlein, C.A. Stan, C.H. Schunck, S.M.F. Raupach, A.J. Kerman, W. Ketterle, *arXiv:cond-mat/0403049*.
- [5] A. E. Muryshev, H. B. van Linden van den Heuvell, and G. V. Shlyapnikov, *Phys. Rev. A* **60**, R2665 (1999); P. O. Fedichev, A. E. Muryshev, G. V. Shlyapnikov, *Phys. Rev. A* **60**, 3220 (1999); Th. Busch and J.R. Anglin, *Phys. Rev. Lett.* **84**, 2298 (2000); J. Dziarmaga, Z. P. Karkuszewski, and K. Sacha, *J. Phys. B* **36**, 1217 (2003).
- [6] S. Burger K. Bongs, S. Dettmer, W. Ertmer, K. Sengstock, A. Sanpera, G. V. Shlyapnikov, and M. Lewenstein, *Phys. Rev. Lett.* **83**, 5198 (1999); J. Denschlag, J. E. Simsarian, D. L. Feder, C. W. Clark, L. A. Collins, J. Cubizolles, L. Deng, E. W. Hagley, K. Helmerson, W. P. Reinhardt, S. L. Rolston, B. I. Schneider, and W. D. Phillips, *Science* **287**, 97 (2000).
- [7] A.L. Fetter and J.D. Walecka, *Quantum Theory of Many-Particle Systems*,
- [8] G. Bruun, Y. Castin, R. Dum, and K. Burnett, *Eur.Phys.J D* **7**, 433 (1999); A. Bulgac and Y. Yu, *Phys.Rev.Lett.***88**, 042504 (2002).
- [9] M. Grasso and M. Urban, *Phys.Rev.A* **68**, 033610 (2003).
- [10] A.J. Heeger, S. Kivelson, J. R. Schrieffer, and W.-P. Su *Rev. Mod. Phys.* **60**, 781-850 (1988).
- [11] M.A. Baranov, *JETP Letters* **70**, 396 (1999).
- [12] G.M. Bruun, P. Törmä, M. Rodriguez, and P. Zoller, *Phys. Rev. A* **64**, 033609 (2001).
- [13] C. Caroli, P. G. de Gennes, and J. Matricon, *Phys. Lett.* **9**, 307 (1964); N.B. Kopnin, G.E. Volovik, and Ü. Parts, *Europhys.Lett.* **32** (1995) 651.